

Carl Schmitt, W. P. Arnott*, and J. Hallett
Desert Research Institute, Reno NV 89506

1. INTRODUCTION

Knowledge of the radiative properties of clouds is important to obtain a more complete understanding of earth's radiation budget. While adequate theoretical models exist for the single scattering properties of ice crystals at solar wavelengths, thermal infrared properties are difficult to obtain because exact solutions of Maxwell's equations are often needed. Laboratory measurements of ice cloud radiative properties are useful for improving the understanding of thermal infrared transfer, and for evaluation of newly developed numerical methods (Yang, et. al., 1997) and approximations.

2. EXPERIMENTAL SETUP

A diagram of the experimental setup is shown in figure 1. The growth chamber and cloud chambers were both cooled to -20°C . An ultrasonic nebulizer was positioned to deliver water drops into the top of the growth chamber. A cloud seeder was placed two meters from the top of the growth chamber. The seeder consisted of a looped spring that was passed through liquid nitrogen, then into the chamber. The cloud chamber was a 1m x 1m x 1.2m interior diameter freezer.

The cloud chamber had a small hole (7.5 cm diameter) in one side for the FTIR to look into, and a large hole (24 cm diameter) on the opposite side. The large hole was covered by a liquid nitrogen cooled conical blackbody. This provided a very low emission background for the experiment. A modified Bomem MB-100 spectrometer was used. Emission measurement calibration was done with software based on Revercomb (1988). Two blackbody cones of known temperature were placed by the FTIR. An uncoated flat gold mirror was used to change the FTIR's field of view from either of the calibration

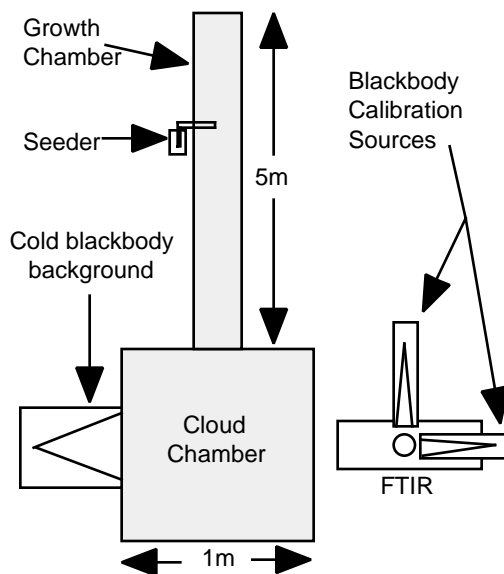


Figure 1. Side view of experimental chamber and FTIR arrangement.

blackbodies to the experimental chamber.

3. PARTICLE OBSERVATION

A new version of a cloudscope described in Arnott (1995) was developed and used to sample the ice crystals. A microscope objective and a compact video camera were used to image crystals. The collection surface was an optical bar of sapphire heated at the sides with a nichrome wire to sublimate ice crystals. The collection surface of the new cloudscope is 1 mm wide, and the incoming air velocity is 3 m/s. The collection efficiency of the cloudscope was estimated using principles from Langmuir (1961) and is shown in figure 2. These collection efficiencies were used only as a guideline for theoretical interpretation.

The temperature of the growth chamber was adjusted to grow different habits of ice crystals (columns and plates).

*Corresponding author address: W. Patrick Arnott, Desert Research Institute, PO Box 60220, Reno, NV 89506. Pat@dri.edu.

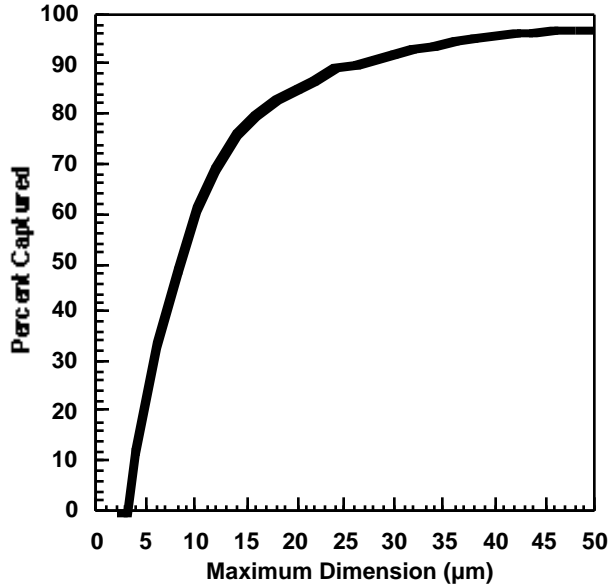


Figure 2: Cloud-scope collection efficiency.

4. RESULTS

Figure 3 shows the infrared emission of with no cloud present. The large feature at 600-700 cm^{-1} is caused by carbon dioxide. The spikes between 1350 and 1750 cm^{-1} are due to water vapor emission, as are the spikes near 500 cm^{-1} . These features are visible on all lab cloud emission spectra. A window region exists between 800-1200 cm^{-1} . The slight rise near 800 cm^{-1} is caused by a small amount of

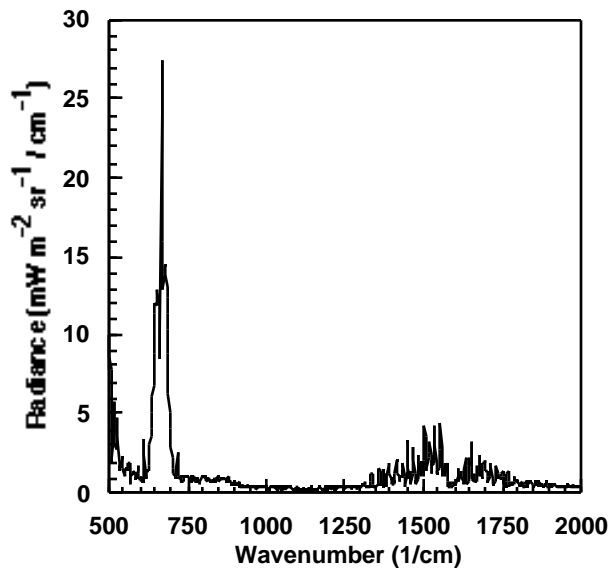


Figure 3: Cloud chamber emission with no cloud present.

cloud that forms near the cold blackbody.

The emission from an ice cloud with an visible optical depth of 0.26 and a temperature of -15°C is shown in figure 4. Carbon dioxide and water vapor emission are clearly present. The underlying smooth curve is due to the ice crystal cloud. The hump that extends from 500 cm^{-1} to 900 cm^{-1} is the main wavenumber range that shows differences with different cloud particles.

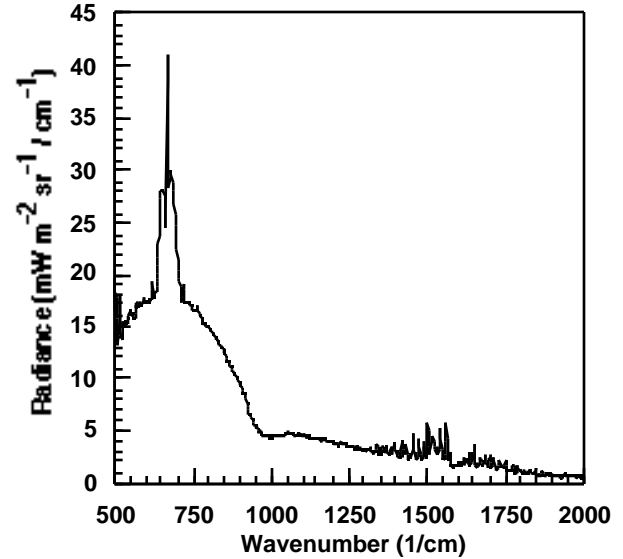


Figure 4: Emission from a lab cloud with an optical depth of 0.26 and a temperature of -15°C .

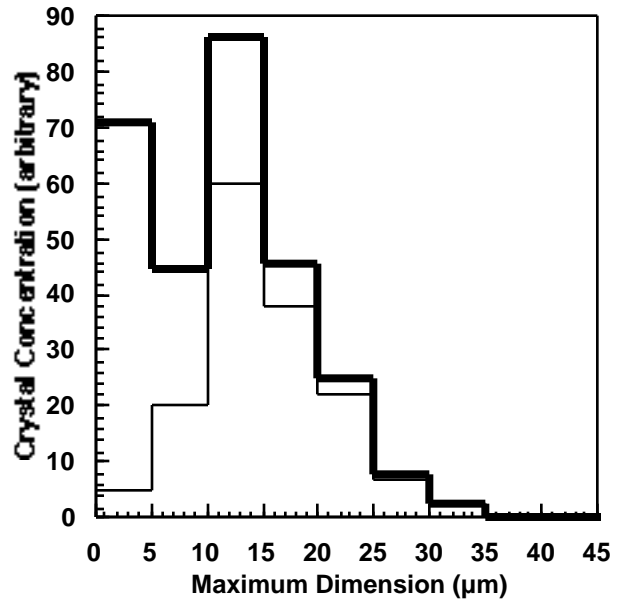


Figure 5: Particle size distribution for the spectra shown in fig 5. Bold(light) lines are the adjusted (raw) data.

The size distribution of the particles captured by the cloudscope at the same time as the measurement was being taken is shown in figure 5. The raw and collection efficiency corrected distributions are shown on the same plot.

5. THEORETICAL ANALYSIS

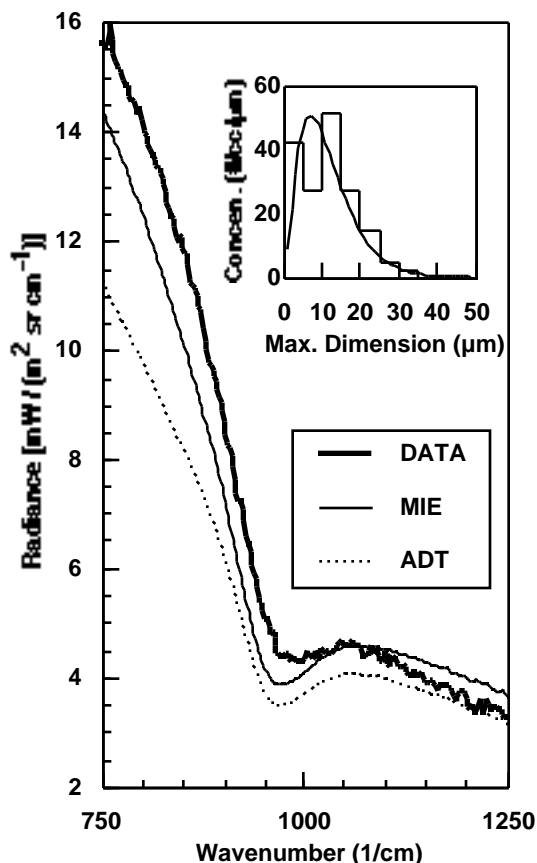


Figure 6. Measured and modeled spectra in the window region. The inset graph shows the gamma distribution fit to the measured size spectra. Plate crystals were assumed in the conversion from hexagonal geometry to spherical.

Theory was adapted from Morrison, et. Al. 1991. Conceptually, the model accounts for emission from the cold blackbody that is attenuated by the cloud (ice crystals, water vapor, and carbon dioxide); emission from the chamber walls that is scattered into the spectrometer field of view by particles; emission by particles in the immediate field of view of the spectrometer; and emission from the cloud that is multiply scattered to the spectrometer field of view. Radiation exiting the chamber is attenuated on passage to the spectrometer by room temperature water vapor

and carbon dioxide, and these gases also emit radiation into the field of view. The numerical model uses CO₂ and H₂O vapor attenuation from the hitran96 data base at a resolution of 0.003 1/cm; a kernel formulation of Mie theory or ADT for particle cross sections where sphere diameter is chosen by conserving the ratio of crystal volume to average projected area; a 3 parameter gamma distribution fit to measured crystal size spectra; a use of a triangular shaped filter function to spectrally average the computation to 4 1/cm resolution. Details will be given elsewhere.

Figure 6 shows measured spectra (same as in Fig. 5), and model results using Mie and ADT theory in the window region. While both theoretical results are not entirely adequate, Mie theory is better than ADT. The measured and gamma size distributions are shown inset. No adjustable parameters are used.

Other data and theory comparisons also show that Mie theory is somewhat adequate if the conversion to spherical geometry conserves the ratio of crystal volume and area.

Acknowledgements: This work was supported by NSF under grant ATM9413437.

6. REFERENCES

- Arnott W. P., Y. Y. Dong, and J. Hallett, 1995: Extinction efficiency in the infrared (2-18 μ m) of laboratory ice clouds: observations of scattering minima in the Christiansen bands of ice. *Appl. Opt.* **34**, 541-551.
- Yang, P., K. N. Liou, and W. P. Arnott, 1997: Extinction efficiency and single scattering albedo for laboratory and natural cirrus clouds. *J. Geophys. Res.* **102**, 21,825-21,835.
- Langmuir I., 1961: The collected Works of Irving Langmuir Vol 10 Atmospheric Phenomena, Pergamom Press, pp. 354-372.
- Morrison, et. Al., 1991: FT-IR spectroscopy in process monitoring Part 1: Theory. *Sensors* **8**, pages unknown.
- Revercomb H. E., et. al., 1988: Radiometric calibration of IR Fourier transform spectrometers: solution to a problem with the High-Resolution Interferometer Sounder. *Appl. Opt.* **27**, 3210-3218.